



# Investigating Blasting Demolition Dust Micromorphology, Microscopic Agglomeration Process With Wetting Droplet and Suppression Effectiveness by Explosion Water Mist

Jiangtao Fu<sup>1,2,3,4</sup>, Lingling Hu<sup>1,2,3\*</sup> and Minghua Hu<sup>4,5</sup>

<sup>1</sup>State Key Lab of Precision Blasting, Jiangnan University, Wuhan, China, <sup>2</sup>Hubei Key Lab of Blasting Engineering, Jiangnan University, Wuhan, China, <sup>3</sup>Hubei (Wuhan) Institute of Explosion Science and Blasting Technology, Jiangnan University, Wuhan, China, <sup>4</sup>Institute of Environment and Health, Jiangnan University, Wuhan, China, <sup>5</sup>Hubei Key Laboratory of Industrial Fume and Dust Pollution Control, Jiangnan University, Wuhan, China

## OPEN ACCESS

### Edited by:

Anthony Chun Yin Yuen,  
University of New South Wales,  
Australia

### Reviewed by:

Timothy Chen,  
University of New South Wales,  
Australia

Cheng Wang,  
University of New South Wales,  
Australia

### \*Correspondence:

Lingling Hu  
linglinghu@jhu.edu.cn

### Specialty section:

This article was submitted to  
Atmosphere and Climate,  
a section of the journal  
Frontiers in Environmental Science

**Received:** 25 February 2022

**Accepted:** 22 June 2022

**Published:** 12 July 2022

### Citation:

Fu J, Hu L and Hu M (2022)  
Investigating Blasting Demolition Dust  
Micromorphology, Microscopic  
Agglomeration Process With Wetting  
Droplet and Suppression Effectiveness  
by Explosion Water Mist.  
Front. Environ. Sci. 10:883386.  
doi: 10.3389/fenvs.2022.883386

Blasting demolition has been widely used in the safe and efficient demolishing of construction buildings. Blasting demolition dust is the most visible and realistic harmful material during the blasting process. The characteristics and suppression of the blasting dust are scarcely addressed in the literature. This article investigated the micromorphology characteristic of blasting demolition dust from a typical building demolition project. The dust median size value D50 was 65.890  $\mu\text{m}$ , and it showed a character of smooth edge, fluffy structure, and cracks. It consists of higher content of heavy metals than conventional cement powder particles, which include Mn, Ni, Zn, and As elements. The dust cannot be wet by municipal water for its hydrophobic character. A novelty method was proposed to set a methodology to form a stable, larger volume, and surface area water droplet on a rod stand, which provided more opportunities to find out and verify the microscopic agglomeration phenomenon and effectiveness between dust and different wetting droplets. The single dust-droplet collision results can be accurately recorded by the high-speed camera with a microscope, the collision and submergence time between blasting demolition dust particle and municipal water droplet on the stand was 2 ms, while the time was 1.125 ms with surfactant solution droplet, which was much shorter than the time of municipal water. The dust-droplet microscopic collision results were shown that the blasting demolition dust can be better wet and agglomerated by a surfactant solution. In blasting demolition projects, the BDD suppression methods with surfactant solution explosion mist have the highest efficiency, which can restrict the BDD's concentration to 10 mg/m<sup>3</sup>.

**Keywords:** blasting demolition dust, precision blasting, high-speed camera, explosion water mist, agglomeration

## 1 INTRODUCTION

With the high speed of urbanization, high-rise buildings, viaducts, and commercial malls are built in cities. Meanwhile, many old or less functional buildings and viaducts need to be demolished in advance. In the limitation of time, safety, and environmental protection, the blasting demolition is superior to traditional methods such as mechanical crushing, cutting, and dismantling (Song et al., 2018). But there are also many adverse effects during the blasting demolition process, such as vibration, flying stones, noise, blasting demolition dust (BDD), and shock wave. Many previous studies on blasting adverse effects are mainly focused on vibration and flying stones (Tsinidis et al., 2016; Xia et al., 2019; Zhang et al., 2021), the rest adverse effects do not receive as much attention. However, BDD is the most visible and realistic harmful material during the blasting demolition process, it is necessary to suppress the dust amount and reduce the complaints of civilians around the blasting demolition site. With the high-speed development of blasting demolition in the urban renewal process, the hazards of BDD are gradually being recognized by the public.

Wetting spray is a common approach for dust suppression in many fields, such as coal mines, building construction, steel mill, lead and zinc mines, and road maintenance (Ma et al., 2018). It utilizes a wet dust remover to spray atomized water into the air, which wets and precipitates the dust particles dispersed in the air, increases their weight and facilitates their settling, to suppress the dust. In other words, to enhance the dust suppression efficiency, it is important to increase the collision probability between dust particles and wetting spray water droplets. In the blasting demolition process, the wetting spray is also widely used as a way to control dust, municipal water is usually used as the wetting material to wet the dust particles and restrict the spread of dust. Chugh et al. (2012) proposed a field assessment of a SIUC innovative spray system for continuous miners for dust control, and the effectiveness of innovative mist spray methods was discussed. Kollipara et al. (2014) found out that spraying atomized water can hardly deliver a satisfactory dust suppression effect, while it is difficult to alter the wettability of the coal dust in practice, the same embarrassment may exist in BDD suppression. Surface properties are critical for dust wettability and suppression efficiency, and the particle size is also important for particle surface wettability (Srikanth et al., 1995; Yang et al., 2010). Gurley et al. (2012) also provided a wet scrubber method to suppress coal dust. Relangi (2012) discussed the wetting characteristics of Herrin coal and its application for improved dust control. Therefore, to find out the suppression efficiency of BDD by water mist, particle surface properties and size should be investigated accordingly.

With the wide application of blasting technology in urban renewal, the requirements for blasting are becoming more and more precise, and dust precision controlling is becoming one of the key tasks in precision blasting (PB). To achieve this goal, there are three major challenges concerning the BDD suppressant in the PB process, including blasting original dust characteristics, high suppression efficiency, and high cost. In this regard, finding out the dust characteristics and the phenomenon of dust wetting

spray suppression can overcome the challenges associated with the conventional municipal water spray method.

To better understand the wettability of dust, many scholars focused on the coal dust characteristics (Xu et al., 2018). Zhang et al. (2020) studied the microscopic phenomenon of several different types of surfactants affecting coal dust wettability based on the nuclear magnetic resonance (NMR) experiments. The results showed that phenol, aryl ether carbon, aliphatic, and aromatic methyl groups are the key parameters affecting coal dust wettability. Xie et al. (2020) found that air moisture, oxygen-containing functional groups, ash, and hydroxyl groups of coal dust can improve the wettability, while the aromatic hydrocarbons weaken the coal dust wettability and affect the synergistic acidification of sodium dodecyl sulfate (SDS) and coal. Wang et al. (2017) investigated the relationship between the contact angle and functional groups obtained by FTIR of respirable coal dust, and concluded that oxygen-containing functional groups are hydrophilic factors and aromatic hydrocarbons and aliphatic hydrocarbons are hydrophobic factors. To the best of our knowledge, by adding surfactants to water before the atomized spray the dust suppression effect can be greatly enhanced (Shah, 1998, Ni et al., 2018). Many mechanisms have been proposed to explain the wettability alteration by surfactants, and it is also verified by engineering projects, but few have been verified and investigated experimentally (Salehi et al., 2008), especially by experiments in micro-scales. Therefore, the objective of this study is to investigate the micro-collision phenomenon of BDD and different wetting agents, municipal water droplets, and to verify the dust suppression effectiveness of blasting demolition projects.

Research on single droplet capture is significant to understanding the phenomenon of dust particle wet deposition in the open atmospheric environment (Bae et al., 2010). Suppression of dust particles by wet deposition is the process of particles captured by water droplets, two stages are composited: movement to the droplet surface under the influence of external forces and movement after impacting on the droplet surface. The impact behavior of micron dust particles on the droplet's surface shows three modes, namely, submergence, oscillation, and rebound (Wang et al., 2015). Usually, the diameter of a scrubbing droplet is over 200 times larger than that of a particle. A collision between a particle and a droplet is similar to that between a particle and a liquid surface (Lee and Kim, 2011). The droplet surface on which the dust particles impact at a certain initial velocity can be considered to be horizontal as tipping stones across the water. Clanet et al. (2004) found out that a certain angle between the stone and the water's surface is optimal to the throwing conditions and yields the maximum possible number of bounces. However, most of these research methods stay in numerical and computer simulation and the results need to be verified by experiments.

In investigating the dust suppression phenomenon of dust particles and water droplets, it is essential to set a stable and large water droplet. Previous studies comprehensively investigated the interactions between solid and pendant water droplet's surfaces (Wong and Tricoli, 2018). Pozrikidis (2012) investigated the stability of sessile and pendant liquid drops, and Kumar et al.

(2020) studied the shape and stability of pendant drops. Many obvious defects of pendant water droplets were found in experiments. First, it can hardly maintain pendant water droplets stay under a stable condition during the collision of dust because of the weak connection between the droplet and upper capillary. Second, the surface area of the droplet cannot reach the largest to increase the collision probability; it is hard to record the collision image between dust particles and droplets.

In this study, the micro-characteristics of BDD were investigated. Then, we proposed a new method to set a stable, larger surface area, and volume water droplets. By designing a dust and droplets collision experiment and obtaining the collision images to obtain a more thorough understanding of the results of the dust and droplet collision process. Then, possible reasons for the dust micromorphology, dust-droplet collision phenomenon, and agglomeration effectiveness were discussed. Finally, to verify the results of micromorphology and agglomeration of blasting demolition dust (BDD) with water droplets, BDD suppression effectiveness by explosion water mist in three blasting demolition projects was monitored and compared.

## 2 MATERIAL AND EXPERIMENTAL SET UP

### 2.1 Materials

The BDD samples were collected from a building demolition project site in central China. The dust samples were collected from the project site using sampling plates. The sampling points were located close to the demolition building at a distance of 10 m. After the demolition process was finished, the samples on sampling plates were collected in clean, labeled polyethylene bags. After collection, the samples were transported to the State Key Laboratory of Precision Blasting (SKLPB).

For comparison of BDD, conventional commercial cement powder samples were collected from the construction material laboratory in SKLPB. To compare the micro-characteristics, the cement powder samples and BDD were subsequently selected for micromorphology analysis and investigation.

To reveal the phenomenon of dust suppression by the wetting spray method, the different liquid was selected to form wetting droplets, namely, NaCl solution in 15% concentration by mass, municipal water, surfactant solution (sodium dodecyl benzene sulfonate) in 0.005% concentration (Kilau and Pahlman, 1987), and hydraulic oil.

### 2.2 Sample Treatment, Micromorphology, and Characteristics Analysis

Both the BDD and cement powder were placed in a glass tray and left to be dried in at a vacuum drying oven for about 12 h at 120°C and stored in a sample cabinet with limited access. These dust samples were used for micromorphology and characteristics analysis.

Particle size distribution was investigated by a laser particle size analyzer (LPSA) to compare the size difference of these samples. The micromorphology of cement powder and BDD samples was checked by using a scanning electron microscope

(SEM), to compare the micro-structure features (Wagner et al., 2017). The BDD was then analyzed for 18 elements by using an energy dispersive XRF spectrometer, which detection limits in mass percentage are given in parentheses. These elements include Na, Mg, Al, Si, P, S, Cl, K, Ca, Ti, Cr, Mn, Fe, Ni, Zn, As, Sr, and Zr. The XRF analysis (Rigaku ZSX Primus II) was carried out in the Hubei Key Laboratory of Industrial Fume and Dust Pollution Control.

### 2.3 Schematic Illustration of Experimental Apparatus

The experiment was mainly carried out in three steps: droplet set up, dust samples sprayed on the droplet surface, and water droplet dropped to the dust layer and recorded the collision phenomenon and agglomeration phenomenon by using an optical microscope and a high-speed camera with a microscopic lens.

The schematics of the experimental apparatus are described in **Figure 1**, it consists of a computer, a high-speed camera with a microscopic lens, a point light source, a polarizing optical microscope with an inside down light source, a droplet stand and a water eject system, water pipette, and glass plate as dust particles stand plate.

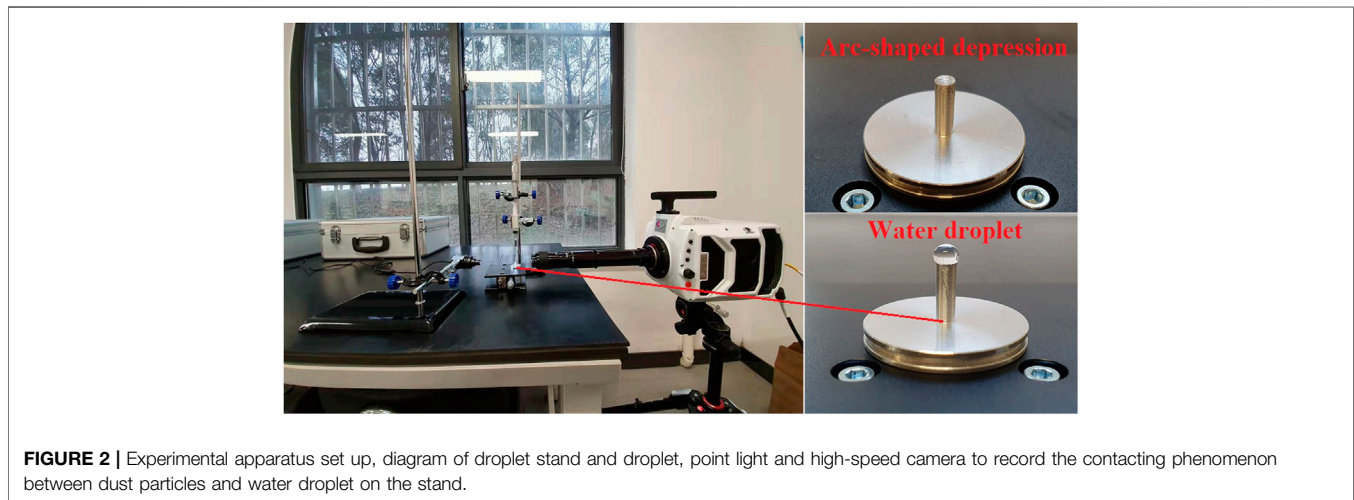
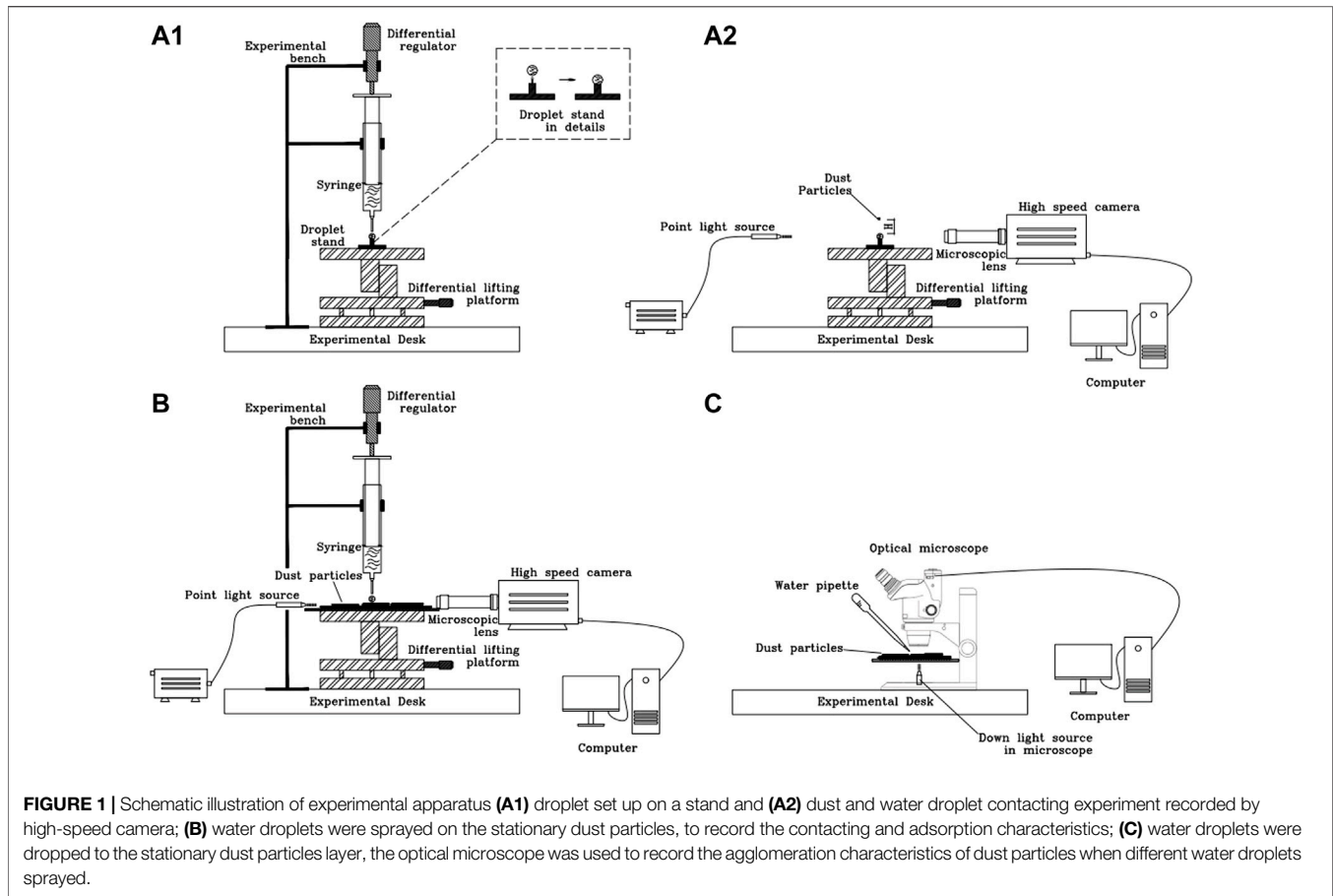
#### 2.3.1 Diagram of Water Droplet and Experiment Apparatus Set up

The differential regulator was set on the upside of the syringe to fine-tune the syringe ejection water volume. The droplet stand was set on the differential lifting platform, the syringe was on the upside of the droplet stand, the diameter of the stand rod was 3 mm. The water samples were dropped from the syringe needle, which was very slow to the droplet stand. To increase the water droplet's surface area, the water from the syringe should be added very slowly to the droplet on the stand. The larger the droplet's surface area, the contact chance between droplet and dust sample can be reinforced. **Figure 1A1** and **Figure 2** show the stand, water droplet, and experiment apparatus set up. To maintain the water droplet staying in a good and stable shape, the stand was rounded into an arc-shaped suppression on the top.

#### 2.3.2 Dust Samples Spray to a Stationary Droplet

In this experiment, the water droplet was set under a stationary condition and dust particles were under a motive condition. Dust particles were collected in a tiny tube, and it was pushed to the droplet without any initial velocity. Dust samples were sprayed onto the droplet by gravity (**Figure 1A2**), where H represents the distance between dust and droplet on the stand. The velocity of dust particles can be calculated according to the H value because of the free-fall motion of dust particles. It was easy to find out the microscopic typical characteristics of single dust and droplet collision at a specific speed.

A high-speed camera with a 12X microscopic lens and a point light source was used to record the shape of the droplet and the dust-droplet collision phenomenon. The droplet on the stand was in the middle between spot light and high-speed camera. The



experiments were carried out under the condition of room temperature of 20°C and relative humidity of 60–80%.

### 2.3.3 Water Droplet Drop to Stationary Dust Particles Layer

Unlike the experiment in 2.3.2, in this experiment, the dust samples were spread on a flat glass plate to form a dust layer,

water droplet was dropped into the dust particles layer. The dust particles were set under a stationary condition and water droplet is under a motive condition in this experiment. In **Figure 1B**, water samples were dropped from the syringe needle very slowly into the dust, to record the contact image between the moving droplet and static dust particles. In **Figure 1C**, water droplet was dropped into the dust from a water pipette, and a polarizing

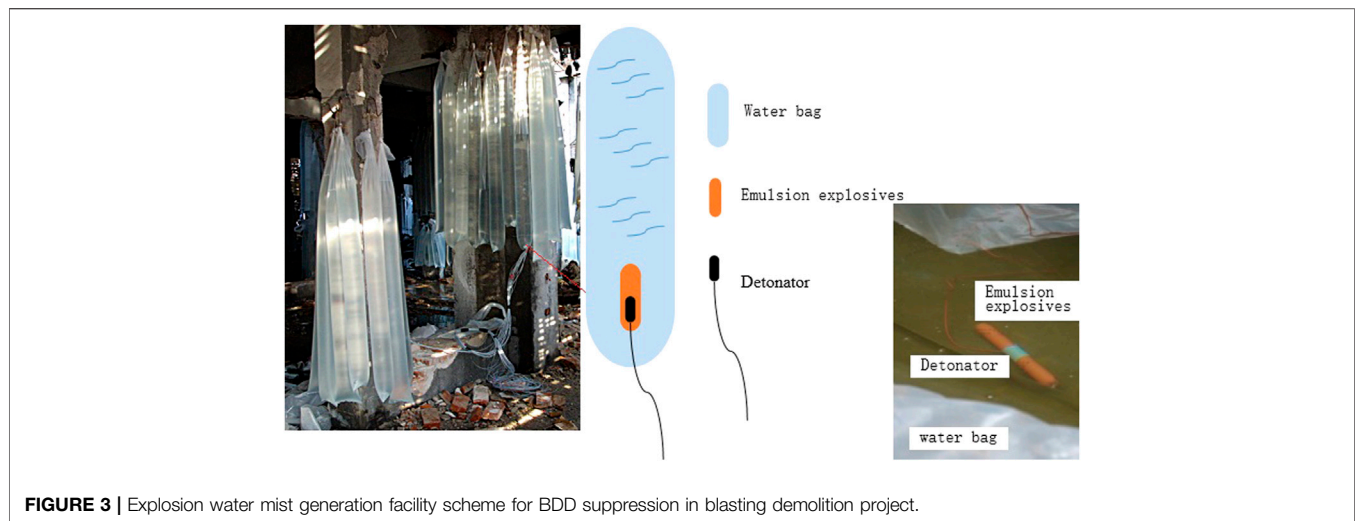


**FIGURE 3** | Explosion water mist generation facility scheme for BDD suppression in blasting demolition project.

microscope was used to record the impacting results of the motive water droplet and stationary dust particles.

## 2.4 Efficiency Comparison of BDD Suppression by Water Mist in Blasting Projects

To verify the efficiency of BDD suppression by different water mists, the generation mode of water mist is one of the key factors. An explosion water mist generation method was created, namely, a water bag, a detonator and the corresponding amount of emulsion explosive were used to form an explosive water mist generation facility. The sample facility schematic is shown in **Figure 3**.

Three different blasting demolition projects' BDD conditions were monitored and compared, which include blasting without the BDD suppression process, BDD suppression with municipal water mist and with surfactant solution mist. The BDD concentration was monitored by Portable Dust Detectors (PDDs) in each project, and the BDD suppression results were discussed in this project. All the three demolition sampling projects were proceeded in the center of China, to obtain accurate comparative data, the BDD concentrations were monitored for 30 min. The trend of BDD concentration in the 30-min sampling time can be better reflected by the reality of using three methods: without suppression, with municipal water, and surfactant.

## 3 RESULTS AND DISCUSSION

### 3.1 Dust Micromorphology and Characterization

#### 3.1.1 Typical Size of Dust Particle Distribution

Particle size distribution obtained by using a laser particle size analyzer (LPSA) for the cement sample and BDD is shown in the square of a logarithmic graph, **Figure 4**. The BDD samples were collected from **Figure 13A**. The most abundant cement powder

particles are around 25  $\mu\text{m}$ , and BDD particles are around 90  $\mu\text{m}$ . These values indicated that the average dust particle diameter of BDD was much larger than the cement powder. The larger size of BDD particles may be due to the detonation force on the hydrated and hardened formed cement blocks. In other words, after the cement is hydrated and hardened to form a cement block, and the blasting dust formed by the detonation force acting on the cement block, this may become the main cause of the characteristics difference between blasting dust and cement powder particles.

**Table.1** shows the characteristics of two samples. The median size of D50 is 23.666  $\mu\text{m}$  for the cement powder sample and 65.890  $\mu\text{m}$  for the BDD sample, 90% cement powder diameter is less than 29.25  $\mu\text{m}$ , and 90% BDD is less than 176.278  $\mu\text{m}$ . Most BDD is a kind of falling dust. The diameter of the cement powder is smaller than that of BDD. The specific surface area S/V values of the cement powder sample are much larger than the BDD sample. A similar trend can be observed in the optics concentration values; this is because aerosols with smaller dust particle sizes will restrict the penetration ability of the laser beam in LPSA operation. These values indicate that there is an essential difference between BDD and cement powder. Obviously, in terms of dust suppression methods, it is not appropriate to simply transplant cement powder suppression methods into BDD. Cement powder is a kind of continuous source of pollution during the cement producing process, and the suppression method is continuous technology. However, the BDD is a kind of instant source of pollution, to suppress BDD, it is a key to create a large amount of mist in a very short time. "Explosion water mist" is created according to this requirement. **Figure 3** to acquire the typical dust and droplet collision experiment results, the BDD was sieved by a 200-mesh (75  $\mu\text{m}$ ) screen for subsequent dust and droplet collision experiments because most of the BDD diameter is below 200 mesh.

#### 3.1.2 Micromorphology of Dust

The surface micromorphology of the cement sample and BDD are observed in the SEM images (**Figure 5**). The dust samples were amplified at 1,700 times by SEM, and the images are all in the same

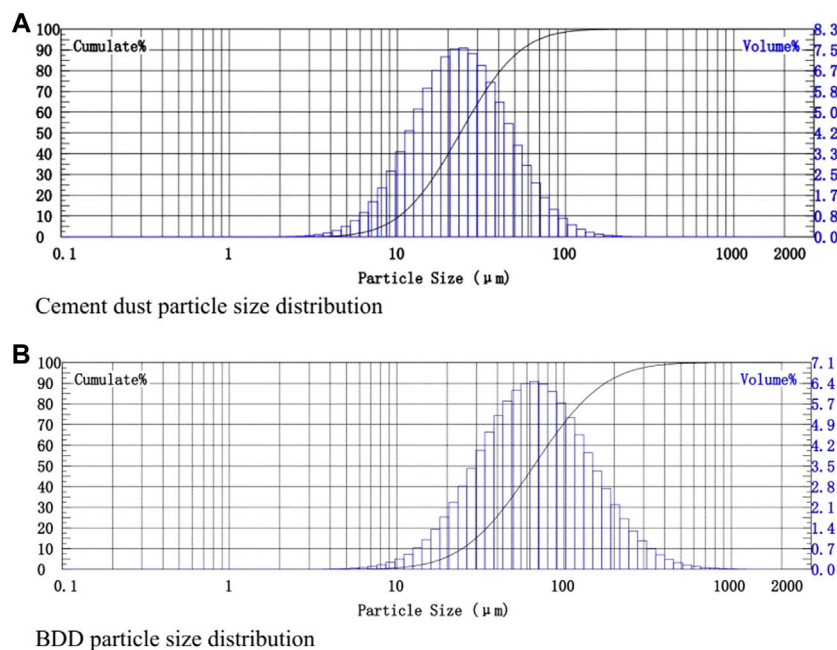


**FIGURE 4** | Dust particle size distribution, (A) cement powder and (B) BDD.

**TABLE 1** | Dust parameters results.

Parameter	Type of dust	
	Cement powder	Blasting demolition dust
D10 ( $\mu\text{m}$ )	10.284	24.625
D50 ( $\mu\text{m}$ )	23.666	65.890
D90 ( $\mu\text{m}$ )	54.449	176.278
Dav ( $\mu\text{m}$ )	29.250	88.512
S/V ( $\text{cm}^2/\text{cm}^3$ )	3134.370	1223.776
Optics Concentration	27.2	15.3
Fit error (%)	0.036	0.031

contrast scales ( $50\ \mu\text{m}$ ). **Figure 5A** shows that cement powder has a sharp edge and no crack structures and exists in each dust particle. **Figure 5B** shows that the BDD samples have a smooth edge, and many cracks existed in dust particles. The typical characteristics of BDD are the main causes of larger porosity than cement powder. The particle diameter information of the two samples has similar characteristics as **Figure 4**.

The structure of blasting demolition particles became looser than cement powder, as seen in **Figure 5B**. The cracks and fluffy construction may be caused by the detonation force in the blasting operation. The micromorphology of cement powder is more stable than that of BDD. When the BDD are contacted with each other or impacted with other materials, they may disintegrate into small pieces because of the fluffy structure, which will increase the concentration of dust in the air.

### 3.1.3 Element Composition of Dust

Results of element determinations of cement powder samples and BDD samples are presented in **Table 2**. The abundances of Si in

cement powder are two times higher than those in the BDD, the widely used cement in China is Portland cement, and the high content of Si is evident. In addition, this may be also evidenced that the dust of demolition blasting is not complete from cement particle dust. Element Ca is nine times and S is 12 times in the BDD than those in cement powder. The abundances of heavy metals, such as Mn, Ni, Zn, and As are also higher in the BDD. However, there is no obvious relationship between the contents of Na, Mg, Ti, and Fe determined by the XRF technique.

The mass percentage of elements Ca and S in the BDD is much higher than that of the cement powder, which may be due to the large number of gray bricks used in the construction of the demolition building, these bricks were produced from flue gas desulfurization (FGD) ash in nearby coal fired power plants (Telesca et al., 2013; Li and Jiang, 2021); in other words, the content of elements Ca and S in the FGD ash (Fu et al., 2018; Fu et al., 2019) is much higher than that of the cement used in the structural column, which leads to this result. Moreover, element Cl has the same characteristics, which is also because of the high concentration in FGD ash (Fu et al., 2018). These values of Na, Mg, Ti, and Fe are rather ambiguous, and it is hard to determine some relationships and draw appropriate conclusions due to the dust sample sources. The widely used coal fire power plants waste increases the migration risk of heavy metals during the blasting demolition process.

### 3.1.4 Wettability of Blasting Demolition Dust

Wetting of BDD is a complicated process involving the interaction among solid, liquid, and gas (three phases). BDD has different porous structures (**Figure 5B**), which may influence the wetting ability of the dust. This experiment was carried out

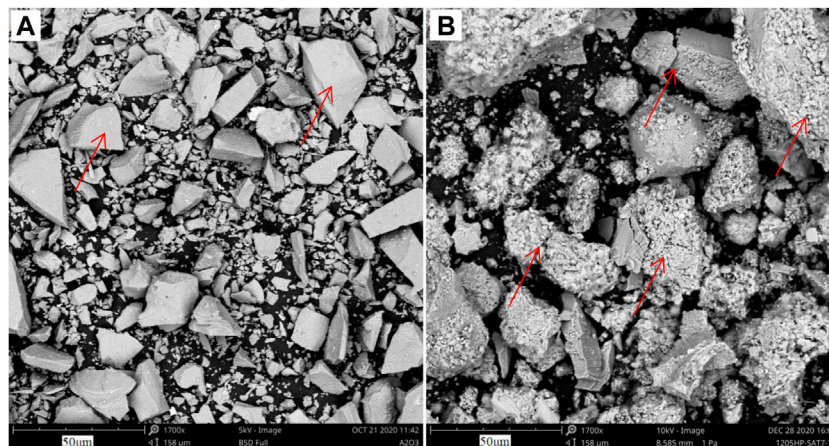


**FIGURE 5** | SEM images of cement powder (A) and BDD samples (B).

**TABLE 2** | Mass concentration of elements of cement powder samples and BDD samples (CH2 represent the mass percentage of other elements other than the indicated 18 elements among elements No. 9-No.92).

Element	Cement powder (mass%)	Blasting demolition dust (mass%)
Na	0.4895	0.191
Mg	1.0892	0.4786
Al	3.9069	2.1577
Si	9.1181	4.6125
P	0.0631	0.0242
S	0.0284	0.3344
Cl	N/A	0.0349
K	1.4607	0.3952
Ca	1.1731	10.5092
Ti	0.1373	0.1098
Cr	0.0115	N/A
Mn	0.0243	0.03
Fe	1.5856	0.6916
Ni	0.0035	0.0045
Zn	0.003	0.0066
As	N/A	0.0044
Sr	0.0043	0.0568
Zr	0.0032	0.0101
CH2	80.89	80.3484

according to **Figure 1B**. **Figure 6** shows the contact angle image of a municipal water droplet and BDD layer on a glass plate, which was a record by high-speed camera.

In **Figure 6**, the contact angle of cement powder is  $89^\circ$ , while BDD is  $84^\circ$ , and the hydrophilicity of cement powder and BDD is similar. Cement powder is a kind of hydrophobic particle because of the smaller particle diameter, and BDD's hydrophobic characteristic may be due to the microporous and fissure structures on the particle surface, which increases the specific surface area of BDD. In addition, there is a layer of air film on the surface of dust particles and water mist, only when there is a high relative movement speed between dust particles and water droplets, do the water droplets break through this layer of air film to capture dust particles, the collision speed may become the dominated factor for dust suppression (Wang et al., 2015).

## 3.2 BDD and Droplets Collision Phenomenon

### 3.2.1 Comparison of Pendant Liquid Droplet and Droplet on the Stand

To compare the difference between pendant liquid droplet and droplet on the stand, municipal water was used to form the two

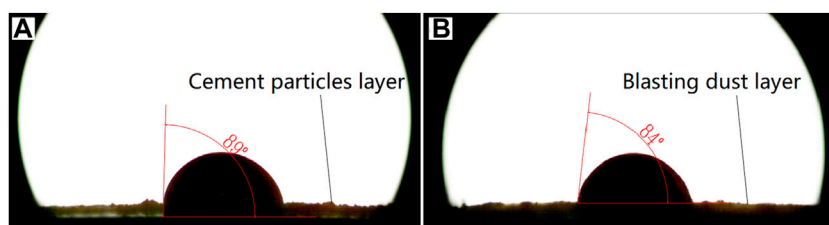


**FIGURE 6** | Contact angle between municipal water droplet and cement powder (A) and BDD (B) layer.

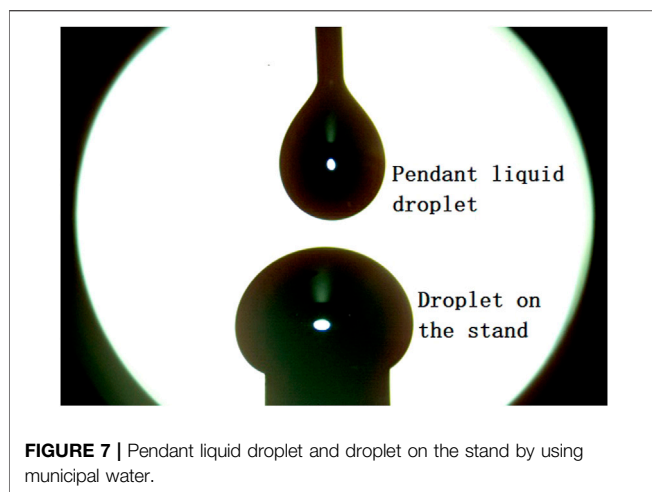


**FIGURE 7** | Pendant liquid droplet and droplet on the stand by using municipal water.

NaCl solution is  $94 \pm 27$  mN/m, water is  $74 \pm 22$  mN/m (Bahadur et al., 2007), and surfactant solution is 49 mN/m (Hajibagheri et al., 2018), and surface tension coefficient of different kinds oil is between 17 mN/m–34 mN/m (Sett et al., 2017). The shapes of these fluid droplets on the stand are shown in **Figure 8**.

The images in **Figure 8** were snapshots in the high-speed camera films, during different fluid droplets almost overflow to the outside of the stand rod. The fluid droplet surface tension decreases from **Figure 8A** to **Figure 8D**, and the size, volume, and surface area of these droplets decreased from the biggest to the smallest. According to the concept of “surface tension,” the liquid surface produces a force that shrinks the surface as much as possible. The radius and radian of each droplet from 1) to 4) decreased accordingly; this is also the evidence of surface tension decreased from 1 to 4 in **Figure 8**.

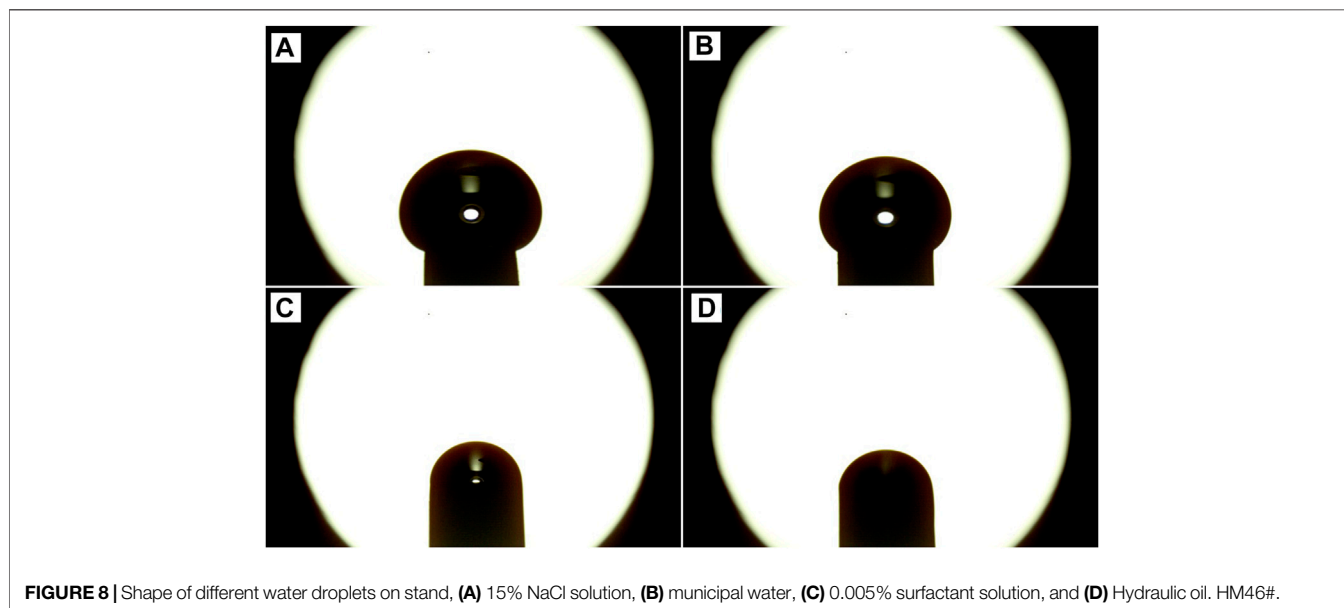


**FIGURE 8** | Shape of different water droplets on stand, (A) 15% NaCl solution, (B) municipal water, (C) 0.005% surfactant solution, and (D) Hydraulic oil. HM46#.

kinds of droplets. The image was recorded by the high-speed camera, in **Figure 7**. To catch the biggest pendant liquid droplet, this image was a snapshot in the high-speed camera films during the pendant liquid droplet almost dropped to the stand. The volume and surface area of the droplet on the stand is much larger than the pendant liquid droplet. The droplet on the stand has much better stability as well. To investigate the collision phenomenon between dust and droplet, the droplet on the stand was chosen to fulfill the following experiments.

### 3.2.2 Shape of Different Water Droplet on the Stand

To find out the relationship between fluid–air surface tension and droplet shape, four kinds of typical fluids with different surface tension coefficients were chosen to form droplets on the stand. It includes 1) 15% NaCl solution, 2) municipal water, 3) surfactant solution, and 4) hydraulic oil HM46#. The surface tension of

Municipal water and 0.005% surfactant solution were chosen as the sample fluid for the further dust and fluid collision experiments. Because municipal water is widely used as the material to control BDD during the demolition process, Sodium dodecyl benzene sulfonate is widely used as a surfactant agent in many industrial fields to suppress dust pollution (Salehi et al., 2008; Shi et al., 2019).

### 3.2.3 BDD and Droplet Collision

Dust and droplet collision experiments were carried out according to **Figure 1A2**, dust particles were dropped to the droplet on the stand at the height of 1 cm, and the collision speed between a single BDD particle and droplet was 0.44 m/s. Ignoring the influence of dust particle size, air resistance, and electrostatic force, only the effect of gravity was considered on dust particles during each experiment. The influence of the surface tension



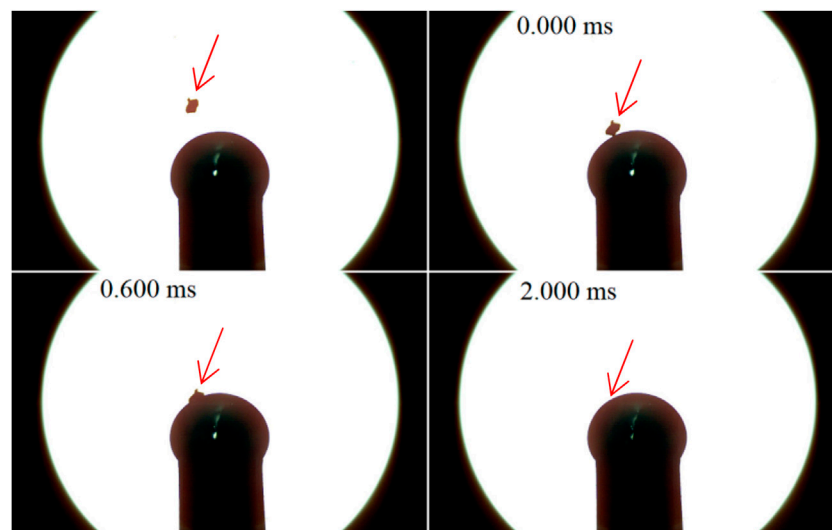


**FIGURE 9** | Blasting demolition dust and municipal water droplets collision results.

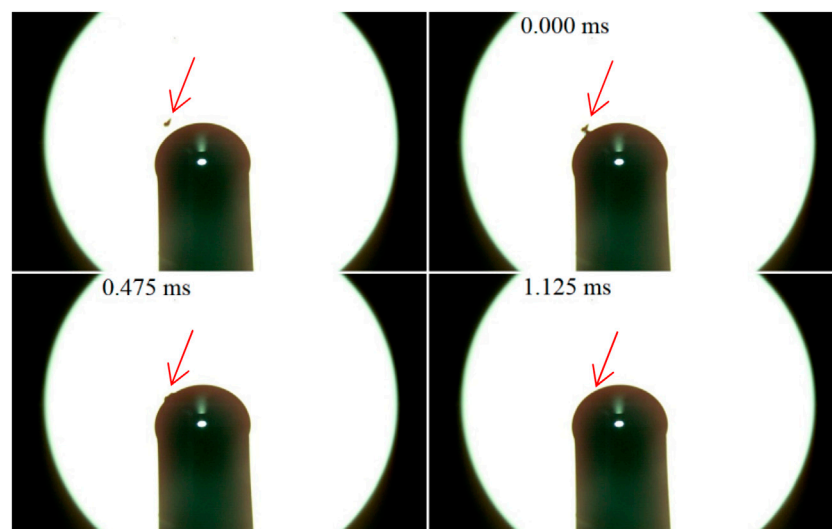


**FIGURE 10** | Blasting demolition dust and surfactant solution droplets collision results.

coefficient and particle size was calculated by the criteria and the following results were found (Wang et al., 2015). As the surface tension coefficient increased from 0.034 N/m to 0.074 N/m, the rebound velocity range changed from 3.96–4.67 m/s to 5.96–7.06 m/s. As the particle size increased from 2  $\mu\text{m}$  to 20  $\mu\text{m}$ , the rebound velocity range changed from 9.69 m/s–11.79 m/s to 2.73 m/s–3.78 m/s. The collision speed of BDD particle and droplet was 0.44 m/s, which was much less than the rebound velocity, the rebound phenomenon would not occur, and all the BDD particles would submerge into the droplets. However, the submergence time would differ according to the surface tension coefficient difference of the droplets.

**Figure 9** shows the collision images of dust and municipal droplets on the stand, and **Figure 10** shows the collision images of dust and surfactant solution on the stand, which can verify the calculation results of Wang et al. (2015).

When the BDD particle first collision with the droplet is recorded as the starting time point, which is 0.000 ms. In **Figure 9**, when the time was 0.600 ms, half of the particle body submerges into the municipal droplet. However, it took another 1.400 ms for the whole particle to submerge into the droplet completely. In **Figure 10**, when the time was 0.475 ms, most of the particle body submerges into the surfactant solution droplet. Moreover, it only took another 0.650 ms for the whole particle to submerge into the droplet completely. The submerge

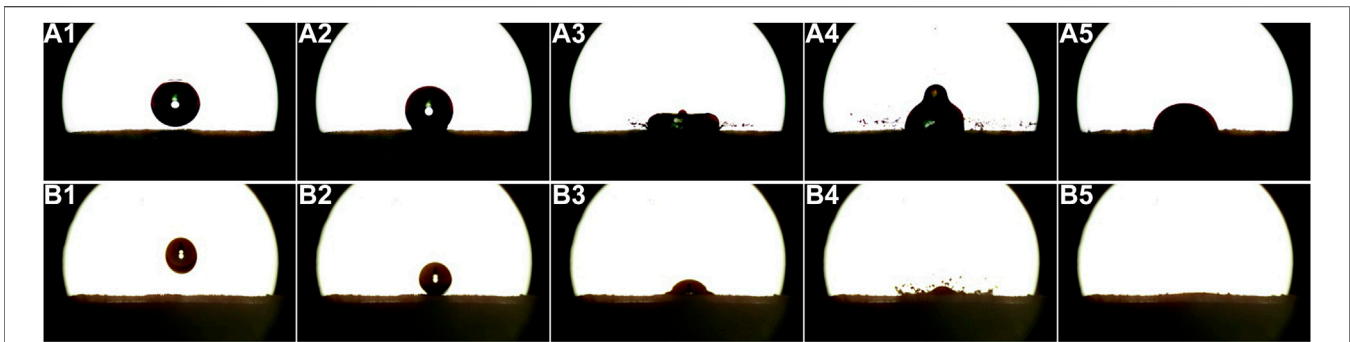


**FIGURE 11** | Agglomeration effect of municipal water (A1–A5) and surfactant solution (B1–B5) drop to the blasting demolition dust layer.

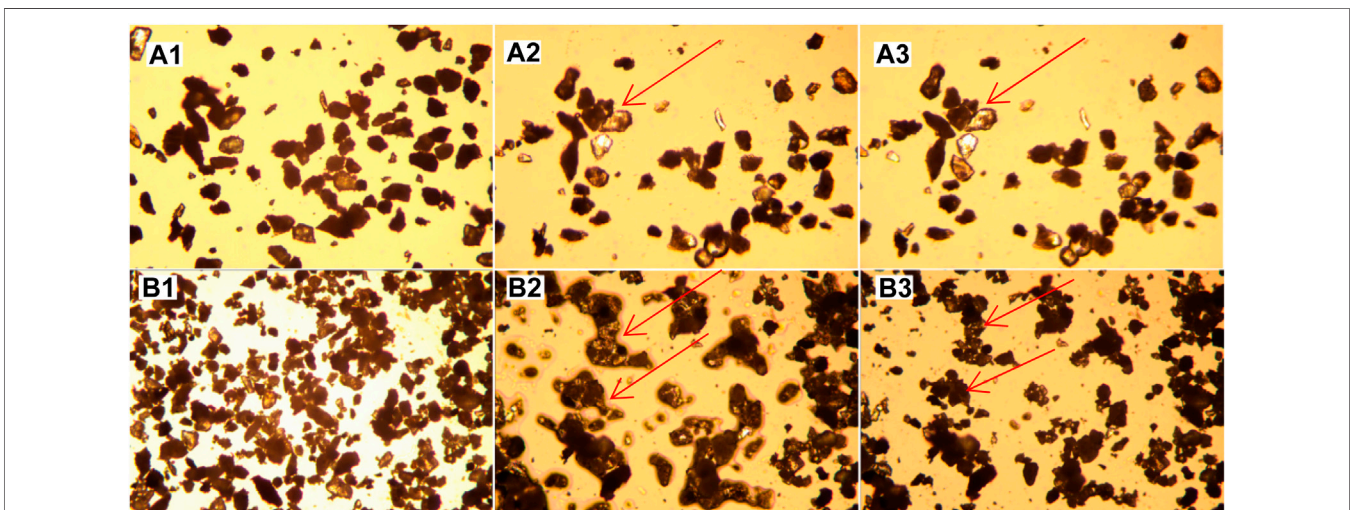


**FIGURE 12** | Agglomeration effect of BDD with municipal water (A1)–initial state, (A2)–after 20 s between water and BDD contacting, and (A3)–ultimate state of agglomeration) and surfactant solution (B1)–initial state, (B2)–after 20 s between surfactant solution and BDD contacting, and (B3)–ultimate state of agglomeration).

time of BDD and surfactant solution droplets collision was only half of the municipal water droplet. It is obvious that there is a significant positive correlation between the contacting time of dust particle droplet and the surface tension; this is also evidenced by the better efficiency of the surfactant in the process of dust particle suppression.

However, the collision and submergence of a dust particle with a droplet as a free-fall mode is only one of the collision types, many other collision phenomena cannot be recorded by this experiment. If the dust particles can be ejected from a different angle with different speeds to collide with the droplet, other contacting images would be recorded, such as oscillation and rebound (Lee and Kim, 2008; Wang et al., 2015). Due to the lack of precision dust aerosol generator instruments, further studies are recommended to identify the contacting angle and velocity affection on the collision results.

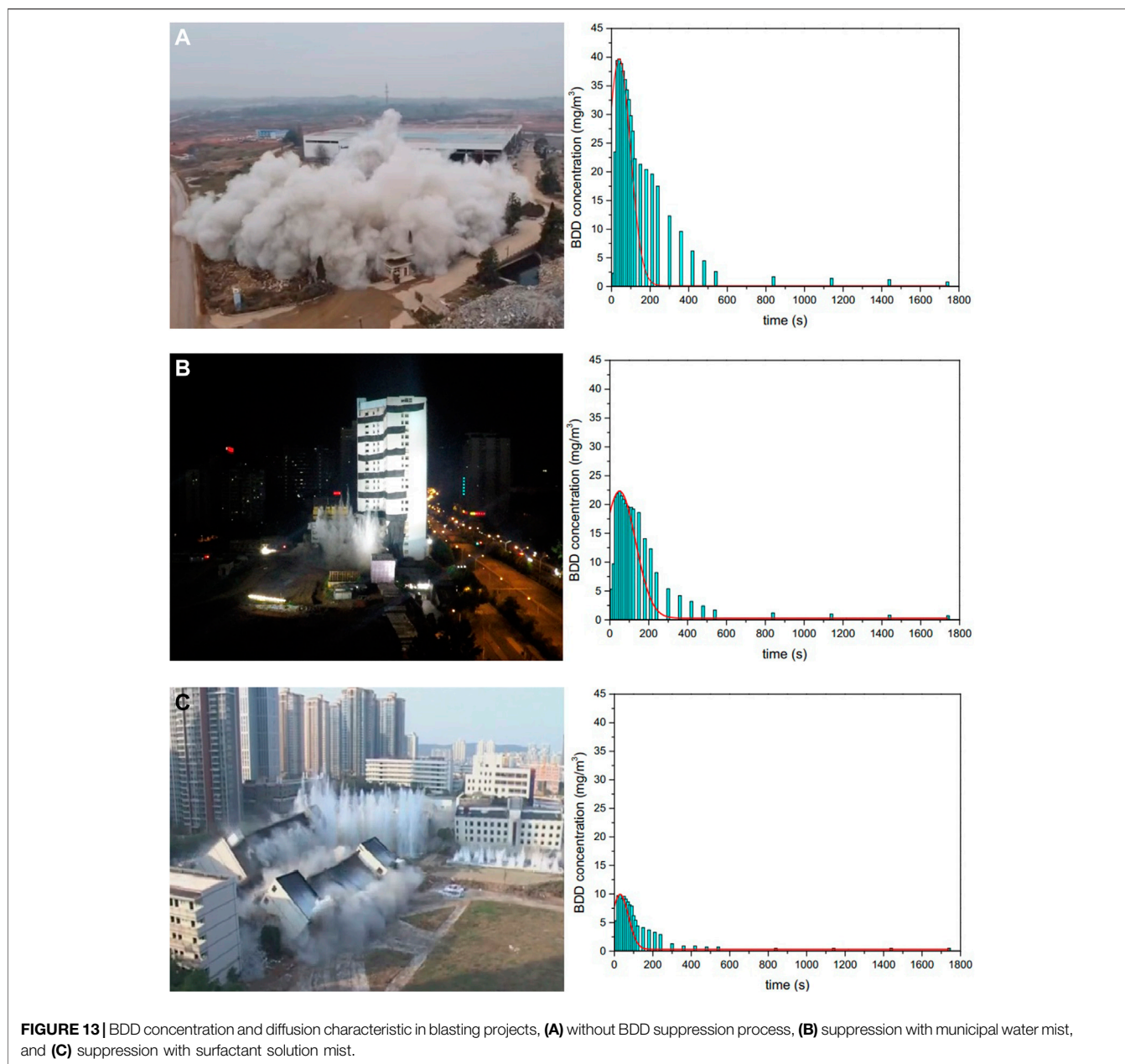
### 3.2.4 Agglomeration Effect of Blasting Demolition Dust With Water and Surfactant

To compare the dust suppression efficiency of municipal water and surfactant, the agglomeration effect should be investigated

(Yuan et al., 2021). These experiments were carried on according to Figure 1B,C.

Agglomeration effect of municipal water Figure 11A1–A5 and surfactant solution in Figure 11B1–B5 drop to the BDD layer. Figure 10A1 and Figure 11B1 show the original images right before the droplet contacted the dust.

Figure 11A2 and Figure 11B2 show the start time of the contact, in Figure 11A3, after 5 ms, municipal water droplets stir up a large number of dust particles on the dust layer, few dust particles adhered to the surface of the droplet. In Figure 11A4, after 10 ms, the wetting condition did not improve, and the dust particles scattered around the droplet irregularly. Finally, in Figure 11A5, the droplets stay in a stable shape, which indicates the hydrophobic characteristic of BDD. In Figure 11B3, no dust particles were stirred up by the surfactant solution droplet. Unlike the municipal water droplet in Figure 11A4, in Figure 11B4 the surfactant solution droplet became flat and dust particles are on the top of the flat surfactant solution, it adhered to the solution surface accordingly. Finally, in Figure 11B5, the dust particles were completely submerged in the surfactant solution. It indicates



that surfactant solution with lower surface tension has stronger agglomeration ability than municipal water for blasting dust.

**Figure 12** shows the BDD condensed by municipal water and surfactant solution. **Figure 12A1** and **Figure 12B1** show the initial dust distribution of the two experiments, which shows that the BDDs were scattered in a state of irregularity.

**Figure 12A2** and **Figure 12B2** show the condition of 20 s after municipal water and surfactant solution dropped into the dust layer. **Figure 12A2** shows the effect of spraying municipal water over the BDD, which indicates that the municipal water sprayed over the BDD can hardly wet the dust. Due to the hydrophobic characteristic of BDD, water tends to flow away or evaporated instead of condensing to the BDD surface. However, in **Figure 12B2**, the effect of spraying surfactant

solution over the BDD, clearly indicates that the BDD is completely wet by surfactant solution, being surrounded by lots of conglomerated liquid particles containing BDD. The BDD condensed together into clumps under the function of surfactant solution, the BDD can be immediately wet and captured by surfactant solution. **Figure 12A3** and **Figure 12B3** show the final agglomeration condition of BDD with municipal water and surfactant solution. After the BDD and municipal water droplet contact, the agglomeration of dust can be neglected. This result is consistent with the wetting result of BDD with municipal water in 3.1.4, which also indicates that BDD is hydrophobic particles to municipal water. Moreover, the agglomeration of dust in **Figure 12B3** is obvious, and the

density of the dust heap is larger. It indicates that the BDD hydrophilic improved with a surfactant solution.

### 3.3 BDD Suppression Affection by Water Mist in Blasting Demolition Projects

To verify the BDD suppression affection by water mist in blasting demolition projects according to the aforementioned experimental results. Three blasting demolition projects were chosen to monitor the BDD concentration and diffusion characteristics, the BDD sampling methods were maintained the same in these projects. **Figure 13** shows the BDD concentration and diffusion results in each blasting demolition project, **Figure 13A** was a project in an outskirts area without any BDD suppression methods. **Figure 13B** and **Figure 13C** projects were implemented in downtown cities, municipal water mist and surfactant solution mist were used to suppress BDD effects.

The change of BDD concentration in **Figure 13A**, **Figure 13B**, and **Figure 13C** indicated that at the initial stage of the emulsion explosives system triggered, the BDD concentration increased straightly. The BDD concentration in **Figure 13A** reach the peak of  $40 \text{ mg/m}^3$ , decreased to  $12.5 \text{ mg/m}^3$  in 300 s, decreased to  $5 \text{ mg/m}^3$  in 480 s, and decreased to  $2 \text{ mg/m}^3$  in 840 s. In **Figure 13B** the concentration reached the peak of  $23 \text{ mg/m}^3$ , decreased to  $5.2 \text{ mg/m}^3$  in 300 s, and decreased to  $1.1 \text{ mg/m}^3$  in 480 s. In **Figure 13C** the concentration reach to the peak of  $10 \text{ mg/m}^3$ , decreased to  $0.9 \text{ mg/m}^3$  in 300 s and decreased to  $1.1 \text{ mg/m}^3$  in 480 s. In blasting demolition projects, the explosion water mist has high efficiency on BDD suppression. The BDD concentration stays at a high level and lasts for a longer time without a suppression method. The surfactant solution mist has the highest BDD suppression efficient, and after 10 min, the BDD vanished entirely in the blasting demolition processing field. Explosion water mist is an efficient method to suppress BDD in blasting demolition projects.

## 4 CONCLUSION

BDD was sampled in a typical building blasting demolition process. The present authors proposed the experiments for the identification of BDD, the results showed that the median size  $D_{50}$  of BDD is  $65.890 \mu\text{m}$ , and it was larger than that of cement powder particles. BDD samples have a smooth edge, many cracks existed in dust particles, and the micro-structure is the main cause of the hydrophobic character of BDD. The chemical composition made them different from cement powder particles, the composition of Mn, Ni, Zn, As, Ca, S, and Cl are significantly enriched in BDD than that of cement, but the abundance of Si in cement particles is two times higher than those in the BDD. The BDD has not totally come from cement powder particles, partially may have come from FGD ash bricks.

This study also verified the micromorphology and characterization results through participle and droplet collision

experiments through high-speed camera with a microscope lens. The time for collision and submerging time between BDD particle and municipal water droplet on the stand was 2 ms, while the time was 1.125 ms between dust particle and surfactant solution droplet. Surfactant solution had better efficiency in the process of dust particle suppression because of its lower surface tension. When the droplet is dropped to the dust particle layer, the BDD cannot be wet by municipal water. In contrast, BDD can be completely wet by surfactant solution, and better agglomeration effect on dust suppression was recorded by surfactant solution. In blasting demolition projects, the BDD suppression methods with surfactant solution explosion mist have the highest efficiency, which can restrict the BDD's highest concentration around  $10 \text{ mg/m}^3$ . Under the premise of project investment control, the use of municipal water with surfactant was the optimal choice for BDD suppression.

However, the collision and submergence between a single dust particle and droplet as a free-fall mode was the only one of the collision type, many other collision phenomena such as different contact angles with different speeds cannot be recorded in this experiment. Further studies are recommended to identify many other possible collision results, which will be more sound and precise for the dust control during the blasting demolition process. This study will be a starting point in the search for dust suppression in the different blasting demolition processes.

## DATA AVAILABILITY STATEMENT

The original contributions presented in the study are included in the article/Supplementary Material; further inquiries can be directed to the corresponding author.

## AUTHOR CONTRIBUTIONS

JF: conceptualization, methodology, writing—original draft, and writing—review and editing. LH: language polishing and editing. MH: XRF analyzing and data curation.

## FUNDING

This work was supported by Key Research and Development Project of Hubei Province, China (grant number 2020BCA084); Research Project of Jiangnan University (grant number 08210057).

## ACKNOWLEDGMENTS

Many thanks also to Hubei Key Laboratory of Industrial Fume and Dust Pollution Control, Jiangnan University.

## REFERENCES

- Bae, S. Y., Jung, C. H., and Kim, Y. P. (2010). Derivation and Verification of an Aerosol Dynamics Expression for the Below-Cloud Scavenging Process Using the Moment Method. *J. Aerosol Sci.* 41, 266–280. doi:10.1016/j.jaerosci.2009.11.006
- Bahadur, R., Russell, L. M., and Alavi, S. (2007). Surface Tensions in NaCl–Water–Air Systems from MD Simulations. *J. Phys. Chem. B* 111, 11989–11996. doi:10.1021/jp075356c
- Chugh, Y., Gurley, H., Kollipara, V., Pulliam, J., Hasenstab, T., Winters, D., et al. (2012). “A Field Assessment of a SIUC Innovative Spray System for Continuous Miners for Dust Control,” in Proc. 14th US/North American Mine Ventilation Symposium, Salt Lake City, UT, June 17–20.
- Clanet, C., Hersen, F., and Bocque, L. (2004). Secrets of Successful Stone-Skipping. *Nature* 427, 29. doi:10.1038/427029a
- Fu, B., Liu, G., Mian, M. M., Sun, M., and Wu, D. (2019). Characteristics and Speciation of Heavy Metals in Fly Ash and FGD Gypsum from Chinese Coal-Fired Power Plants. *Fuel* 251, 593–602. doi:10.1016/j.fuel.2019.04.055
- Fu, J., Hu, N., Yang, Z., and Wang, L. (2018). Experimental Study on Zero Liquid Discharge (ZLD) of FGD Wastewater from a Coal-Fired Power Plant by Flue Gas Exhausted Heat. *J. Water Process Eng.* 26, 100–107. doi:10.1016/j.jpwe.2018.10.005
- Gurley, H., Kollipara, V., and Chugh, Y. (2012). “An Experimental Study of Approaches to Minimize Pressure Loss within Wet Scrubber and Their Effect on Coal Dust Control,” in Proc. 14th US/North American Mine Ventilation Symposium.
- Hajibagheri, F., Hashemi, A., Lashkarbolooki, M., and Ayatollahi, S. (2018). Investigating the Synergic Effects of Chemical Surfactant (SDBS) and Biosurfactant Produced by Bacterium (*Enterobacter C*) on IFT Reduction and Wettability Alteration during MEOR Process. *J. Mol. Liq.* 256, 277–285. doi:10.1016/j.molliq.2018.02.020
- Kilau, H. W., and Pahlman, J. E. (1987). Coal Wetting Ability of Surfactant Solutions and the Effect of Multivalent Anion Additions. *Colloids Surfaces* 26, 217–242. doi:10.1016/0166-6622(87)80118-x
- Kollipara, V. K., Chugh, Y. P., and Mondal, K. (2014). Physical, Mineralogical and Wetting Characteristics of Dusts from Interior Basin Coal Mines. *Int. J. Coal Geol.* 127, 75–87. doi:10.1016/j.coal.2014.02.008
- Kumar, A., Gunjan, M. R., Jakhar, K., Thakur, A., and Raj, R. (2020). Unified Framework for Mapping Shape and Stability of Pendant Drops Including the Effect of Contact Angle Hysteresis. *Colloids Surfaces A Physicochem. Eng. Aspects* 597, 124619. doi:10.1016/j.colsurfa.2020.124619
- Lee, D.-G., and Kim, H.-Y. (2008). Impact of a Superhydrophobic Sphere onto Water. *Langmuir* 24, 142–145. doi:10.1021/la702437c
- Lee, D.-G., and Kim, H.-Y. (2011). Sinking of Small Sphere at Low Reynolds Number through Interface. *Phys. Fluids* 23, 072104. doi:10.1063/1.3614536
- Li, C., and Jiang, L. (2021). Effect of Flue Gas Desulfurization Gypsum Addition on Critical Chloride Content for Rebar Corrosion in Fly Ash Concrete. *Constr. Build. Mater.* 286, 122963. doi:10.1016/j.conbuildmat.2021.122963
- Ma, Y., Zhou, G., Li, S., and Ding, J. (2018). Synthesis and Properties of a Conglomeration-Wetting Spray Agent for Dust Suppression. *Ind. Eng. Chem. Res.* 57, 13940–13951. doi:10.1021/acs.iecr.8b03241
- Ni, G., Li, Z., and Xie, H. (2018). The Mechanism and Relief Method of the Coal Seam Water Blocking Effect (WBE) Based on the Surfactants. *Powder Technol.* 323, 60–68. doi:10.1016/j.powtec.2017.09.044
- Pozrikidis, C. (2012). Stability of Sessile and Pendant Liquid Drops. *J. Eng. Math.* 72, 1–20. doi:10.1007/s10665-011-9459-3
- Relangi, D. D. (2012). Wetting Characteristics of Herrin Coal and its Application for Improved Dust Control. Thesis.
- Salehi, M., Johnson, S. J., and Liang, J.-T. (2008). Mechanistic Study of Wettability Alteration Using Surfactants with Applications in Naturally Fractured Reservoirs. *Langmuir* 24, 14099–14107. doi:10.1021/la802464u
- Sett, S., Yan, X., Barac, G., Bolton, L. W., and Miljkovic, N. (2017). Lubricant-Infused Surfaces for Low-Surface-Tension Fluids: Promise versus Reality. *ACS Appl. Mat. Interfaces* 9, 36400–36408. doi:10.1021/acsami.7b10756
- Shi, G.-Q., Han, C., Wang, Y.-m., and Wang, H.-T. (2019). Experimental Study on Synergistic Wetting of a Coal Dust with Dust Suppressant Compounded with Noncationic Surfactants and its Mechanism Analysis. *Powder Technol.* 356, 1077–1086. doi:10.1016/j.powtec.2019.09.040
- Shah, V. V. (1998). High Performance Wetting Agents Based on Acetylenic Glycol Chemistry. *Adhesive Age* 41, 36–41.
- Song, G., Zhong, M.-S., Wang, M., Long, Y., Liu, Y., and Xu, J.-I. (2018). Collapse Process and Impact Effect of Viaduct Demolition Based on Centrifugal Model. *Soil Dyn. Earthq. Eng.* 115, 246–251. doi:10.1016/j.soildyn.2018.07.034
- Srikanth, R., Zhao, R., and Ramani, R. V. (1995). “Relationships between Coal Properties and Respirable Dust Generation Potential,” in Proc. 7th United States Mine Ventilation Symposium, Lexington, KY, USA.
- Telesca, A., Marroccoli, M., Calabrese, D., Valenti, G. L., and Montagnaro, F. (2013). Flue Gas Desulfurization Gypsum and Coal Fly Ash as Basic Components of Prefabricated Building Materials. *Waste Manag.* 33, 628–633. doi:10.1016/j.wasman.2012.10.022
- Tsinidis, G., Pitilakis, K., and Madabhushi, G. (2016). On the Dynamic Response of Square Tunnels in Sand. *Eng. Struct.* 125, 419–437. doi:10.1016/j.engstruct.2016.07.014
- Wagner, A. C., Bergen, A., Brilke, S., Bühner, B., Ebert, M., Haunold, W., et al. (2017). Characterization of Aerosol Particles Produced by a Skyscraper Demolition by Blasting. *J. Aerosol Sci.* 112, 11–18. doi:10.1016/j.jaerosci.2017.06.007
- Wang, A., Song, Q., and Yao, Q. (2015). Behavior of Hydrophobic Micron Particles Impacting on Droplet Surface. *Atmos. Environ.* 115, 1–8. doi:10.1016/j.atmosenv.2015.05.053
- Wang, H., Zhang, L., Wang, D., and He, X. (2017). Experimental Investigation on the Wettability of Respirable Coal Dust Based on Infrared Spectroscopy and Contact Angle Analysis. *Adv. Powder Technol.* 28, 3130–3139. doi:10.1016/j.apt.2017.09.018
- Wong, W. S. Y., and Tricoli, A. (2018). Cassie-Levitated Droplets for Distortion-Free Low-Energy Solid-Liquid Interactions. *ACS Appl. Mat. Interfaces* 10, 13999–14007. doi:10.1021/acsami.8b00641
- Xia, Y., Jiang, N., Zhou, C., and Luo, X. (2019). Safety Assessment of Upper Water Pipeline under the Blasting Vibration Induced by Subway Tunnel Excavation. *Eng. Fail. Anal.* 104, 626–642. doi:10.1016/j.engfailanal.2019.06.047
- Xie, H. C., Ni, G. H., Xie, J. N., Cheng, W. M., Xun, M., Xu, Y. H., et al. (2020). The Effect of SDS Synergistic Composite Acidification on the Chemical Structure and Wetting Characteristics of Coal. *Powder Technol.* 367, 253–265. doi:10.1016/j.powtec.2020.03.056
- Xu, G., Chen, Y., Eksteen, J., and Xu, J. (2018). Surfactant-Aided Coal Dust Suppression: A Review of Evaluation Methods and Influencing Factors. *Sci. Total Environ.* 639, 1060–1076. doi:10.1016/j.scitotenv.2018.05.182
- Yang, J., Wu, X., Gao, J., and Li, G. (2010). Surface Characteristics and Wetting Mechanism of Respirable Coal Dust. *Min. Sci. Technol.* 20, 365–371. doi:10.1016/S1674-5264(09)60209-X
- Yuan, W., Liao, Z., He, K., Liu, Q., and Huang, S.-M. (2021). An Experimental Investigation on Condensation-Induced Self-Cleaning of Dust on Superhydrophobic Surface. *Appl. Surf. Sci.* 566, 150702. doi:10.1016/j.apsusc.2021.150702
- Zhang, H., Nie, W., Yan, J., Bao, Q., Wang, H., Jin, H., et al. (2020). Preparation and Performance Study of a Novel Polymeric Spraying Dust Suppression Agent with Enhanced Wetting and Coagulation Properties for Coal Mine. *Powder Technol.* 364, 901–914. doi:10.1016/j.powtec.2019.10.082
- Zhang, Z., Zhou, C., Remennikov, A., Wu, T., Lu, S., and Xia, Y. (2021). Dynamic Response and Safety Control of Civil Air Defense Tunnel under Excavation Blasting of Subway Tunnel. *Tunn. Undergr. Space Technol.* 112, 103879. doi:10.1016/j.tust.2021.103879

**Conflict of Interest:** The authors declare that the research was conducted in the absence of any commercial or financial relationships that could be construed as a potential conflict of interest.

**Publisher’s Note:** All claims expressed in this article are solely those of the authors and do not necessarily represent those of their affiliated organizations, or those of the publisher, the editors, and the reviewers. Any product that may be evaluated in this article, or claim that may be made by its manufacturer, is not guaranteed or endorsed by the publisher.

Copyright © 2022 Fu, Hu and Hu. This is an open-access article distributed under the terms of the Creative Commons Attribution License (CC BY). The use, distribution or reproduction in other forums is permitted, provided the original author(s) and the copyright owner(s) are credited and that the original publication in this journal is cited, in accordance with accepted academic practice. No use, distribution or reproduction is permitted which does not comply with these terms.